Complexes of Group II_b Metals with Dithiooxamides.
III. Vibrational Spectra and Thermal Analysis of the $HgLX_2$ Complexes

P. GEBOES* and H. O. DESSEYN

University of Antwerp, RUCA, Laboratory of Inorganic Chemistry, Groenenborgerlaan 171, B-2020 Antwerp (Belgium)

(Received December 5, 1988)

Abstract

In acid or alcoholic media, HgX_2 forms non-electrolyte $HgLX_2$ (X = Cl, Br, I) complexes with dithiooxamides. The ligands act as bidentates with S,S-coordination.

A thorough vibrational analysis (IR and Raman) has been performed for the $Hg(H_2NCSCSNH_2)X_2$ (X = Cl, Br), the $Hg(CH_3NHCSCSNHCH_3)X_2$ (X = Cl, Br) and the $Hg[(CH_3)_2NCSCSN(CH_3)_2]X_2$ (X = Cl, Br, I) complexes, by NH/ND and CH_3/CD_3 isotopic substitution. Monomeric pseudotetrahedral and polymeric octahedral stereochemistries are proposed based on spectroscopic evidence.

Special attention has been given to solid state reactions of the complexes with the KX matrix and also the thermal properties of the complexes have been the subject of this investigation.

Introduction

It has been previously reported [1–3] that Hg(II) forms $Hg(RR'NCSCSNRR')X_2$ (R = H, alkyl; R' = H, alkyl; X = Cl, Br, I) complexes with dithiooxamides in acid media. These complexes can also be formed in ethanolic medium. For the $Hg(NN'DMDTO)X_2$ complexes (R = H, R' = CH_3) the authors proposed a S,N-coordination. The bands in the 390–330 and 330–320 cm^{-1} regions were assigned to νHgN and νHgS vibrations respectively and only some fundamentals were mentioned.

The behaviour of our ligands with group II_b metals is of interest because it is known that the tendency of these metals to coordinate to nitrogen atoms diminishes very markedly on passing from zinc to mercury while the tendency to coordinate via the sulphur atom increases. However, the crystal structure of $Zn(NN'DMDTO)Cl_2$ has recently been determined and shows that NN'DMDTO acts as an S,S-chelating agent. Therefore, knowing that mercury(II) is a typical soft electron pair acceptor forming strong bonds with covalent character to soft donor atoms, the ligands will certainly act as bidentates with S,S-coordination to form $HgLX_2$ complexes.

A thorough investigation of the vibrational spectra (IR and Raman) of the complexes is proposed and special attention has been given to the hydrogen bonding as the series of products seems particularly suitable, since ligands ranging from non-substituted to tetra-substituted could be obtained.

Just as was the case for the $Zn(NN'DMDTO)Cl_2$ complex, solid state reactions of the Hg(II) complexes with the KX matrix have to be considered.

The thermal behaviour of the $HgLX_2$ complexes has also been studied using isothermal and non-isothermal techniques.

Experimental

The complexes were prepared by adding dropwise 1 mmol ligand dissolved in a few ml ethanol to 1 mmol HgX_2 dissolved in a few ml ethanol (or concentrated acetic acid). After precipitation, the complexes were filtered off and washed with ethanol.

The IR spectra were recorded on a Bruker 113v FT spectrometer in a KX matrix (X depends on the complex) in the 4000–400 cm^{-1} region and in a polyethylene matrix in the 500–50 cm^{-1} region.

The Raman spectra were recorded on a SPEX Model 1403, 0.85 m double spectrometer, equipped with a Spectra-Physics Model 2020 argon ion laser: a spinning cell sample holder was used to avoid thermal degradation of the coloured compounds. The excitation was provided by the 514.5 nm line with a laser power of 40 to 300 mW, depending on the complex, at a resolution of 2 cm^{-1} and signal recording was done using photon counting with an integration time of 1 s.

Thermal analysis data have been obtained from a Dupont R90 instrument equipped with a 951 thermogravimetric analyser in a N_2 gas flow (50 ml/min). To obtain the apparent activation energy for the decomposition processes, TG experiments were

---

*Author to whom correspondence should be addressed.

0020-1693/89/$3.50

performed at 20, 10, 5 and 1° min^{-1} using nominally the same sample size of ±3 mg. Sample sizes of 20 to 30 mg were used when the intermediate products were needed for determination.

Results and Discussion

Table 1 summarizes the theoretical and experimental metal percentages, as well as the colours of the complexes. Notice that the iodo-complexes with DTO and NN'DMDTO could not be prepared.

The complexes are microcrystalline or powderlike, stable in atmospheric conditions and insoluble in water, ethanol, acetone, ether, chloroform and benzene. The complexes dissociate in DMSO and DMF.

TABLE 1. Metal analysis (%) and colours of the prepared complexes

Complexes	Hg (%)		Colour
	Found	Calculated	
$Hg(DTO)Cl_2$	48.2	51.2	yellow
$Hg(DTO)Br_2$	38.9	41.8	yellow
$Hg(NN'DMDTO)Cl_2$	47.7	47.8	orange
$Hg(NN'DMDTO)Br_2$	37.4	39.5	orange
$Hg(TMDTO)Cl_2$	44.7	44.8	white
$Hg(TMDTO)Br_2$	36.4	37.4	white
$Hg(TMDTO)I_2$	31.5	31.8	pale yellow

Vibrational Spectra of the Complexes

Hg(NN'DMDTO)X_2

The assignments for the $Hg(CH_3NHCSCSNHCH_3)X_2$ (X = Cl, Br) and for the CH_3/CD_3, NH/ND and CH_3,H/CD_3,D substituted analogues are gathered in Tables 2 and 3. The νNH bands shift to lower wavenumbers on CH_3/CD_3 substitution and on deuteration.

The ratio νNH/νND = (1.33 ± 0.02) indicates a pure NH mode. The association of the N–H proton with the halogen of the neighbour molecule is demonstrated in the position of the νNH stretching modes and more distinctly in the position of the πNH deformation modes of the Cl and Br complexes respectively. The πNH deformations for the Cl complex at 807 and 727 cm^{-1} shift to 782 and 702 cm^{-1} respectively for the Br complex. The πND modes for the Cl complex appear at 562 and 502 cm^{-1} respectively. In accordance with previous results [4–6] the lower νNH corresponds with the higher πNH. This indicates a stronger association for the Cl complex, giving rise to a larger contribution of the polar resonance form to the structure of the thioamide function for the Cl complex.

The νCN band at 1549 cm^{-1} for the Cl complex shifts to 1542 cm^{-1} for the Br complex. This band shifts to 1536 cm^{-1} for the CD_3 derivative, to 1521 cm^{-1} for the deuterated compound and to 1508 cm^{-1} for the CD_3/ND compound.

The bands in the 1470–1400 cm^{-1} region disappear on CH_3/CD_3 substitution and can be assigned to δCH_3 deformations.

The band in the 1380–1370 cm^{-1} region, for the CH_3/Cl complex, which is hardly influenced by Cl/Br and CH_3/CD_3 substitution, shifts to 931 cm^{-1} on deuteration and can be assigned to a δNH deformation.

The very weak bands in the 1300–1200 cm^{-1} region are overtones.

The band at 1209 cm^{-1} for the CH_3/NH complex, which shifts slightly to 1201 cm^{-1} on deuteration, shifts to 1177 cm^{-1} on CH_3/CD_3 substitution and to 1160 cm^{-1} for the CD_3/ND analogue, due to the mass effect. This band has predominantly νNR character.

In accordance with the assignments of the $ZnLX_2$ complexes [4], the band at 1093 cm^{-1} can be assigned to a νCC vibration.

The other bands in the 1200–850 cm^{-1} region are ρCH_3, δCD_3 and ρCD_3 deformations. The band at 873 cm^{-1} shifts to 850 cm^{-1} for the ND derivative, to 847 cm^{-1} for the CD_3 derivative and to 845 cm^{-1} for the CD_3/ND derivative. This band has predominantly νCS character.

The bands in the 700–500 cm^{-1} region, that don't shift on any substitution, can be assigned to ring vibrations. The strong band at 634 cm^{-1} (Raman as well as IR) exhibits no shift by halogen exchange and shifts about 30 cm^{-1} to lower frequencies on CH_3/CD_3 substitution and about 5 cm^{-1} on NH/ND substitution. This band is a δNCS deformation and has probably νCS contribution.

The bands in the 600 cm^{-1} region and the bands in the 390 cm^{-1} region shift only on CH_3/CD_3 substitution and can be assigned to δNR and πNR deformations respectively.

The νHg–S vibrations in the 350–320 cm^{-1} region are assigned according to the literature data [1]. The bands at 267 and 244 cm^{-1} shift to 171 and 142 cm^{-1} respectively on Cl/Br substitution. These bands are hardly influenced by any other substitution and have νHgX character.

Hg(DTO)X_2

Table 4 summarizes the IR and Raman data and the assignments of the $Hg(NH_2CSCSNH_3)X_2$ (X = Cl, Br) complexes and their deuterated derivatives. In contradiction with the results of the $Pd(DTO)X_2$ (X = Cl, Br) complexes [6] there are differences in association strength between the Cl and the Br complexes. This can be deduced from the position of the νNH_2, δNH_2 and ρNH_2 vibrations. The νNH_2 vibrations for the Cl complex at 3186 and 3036 cm^{-1} shift

TABLE 2. Vibrational analysis of the Hg(NN'DMDTO)X_2 complexes

X = Cl		X = Br		Assignment
IR	Raman	IR	Raman	
3155vs	3156vwvbr	3173vs		νNH
3059s	3027w	3059s		νNH
2964m–s	2967w	2959m–s		νCH_3
	2924m			νCH_3
2899w		2894w		νNH
1549vs	1545vs	1542vvs	1540	νCN
1477sh		1464sh		δCH_3
1440sh	1443w	1439sh		δCH_3
1430m	1431w–m	1429m		δCH_3
		1398w		δCH_3
1376m		1372s		δNH
1361w	1365vvs	1359w–m	1362	δCH_3
1265vw	1269vw	1265w		2 × (δNCS + νCS)
1209m	1211sh	1208m	1211	νNR
1201m	1202m–s	1201m		νNR
1168w	1167w	1167w		νNR
1093s	1092vs	1093vs	1093	νCC
1063w–m	1063vw	1060m		ρCH_3
1021m	1020w	1018s		ρCH_3
873w–m	875w	872m		νCS
		808w		
807w–mbr	806vwbr	782w–mbr		πNH
727mbr		702m–sbr		πNH
675w	674w–m	675sh	673sh	ring vib.
634s	634m–s	634s	633s	δNCS + νCC
603w	604w	602w		δNR
	529w		529w	
391w–m	391w	389m	391w	πNR
346w–m	340sh	340m	338sh	νHgS
333w	336w	322w	328w	ring def.
267m	262w–m			νHgCl
244m	254sh			νHgCl
189vw	188w			
		171s	172s	νHgBr
148m	155w			lattice modes
		142m		νHgBr
106m	105sh	106m	101m	lattice modes
81w–m	81vvs	81m	89m	
		64m	57vvs	

to 3243 and 3142 cm^{-1} respectively for the Br complex. The νND_2 bands for the Cl complex appear at 2423 and 2249 cm^{-1} respectively. The δNH_2 and ρNH_2 deformations at 1635 and 1181 cm^{-1} respectively for the Cl complex shift to 1614 and 1174 cm^{-1} for the Br complex. The $\omega,\tau NH_2$ deformation at 739 cm^{-1} shifts to 693 cm^{-1} on Cl/Br substitution. These shifts are in accordance with the reasoning that the Cl complexes have stronger associations than the Br complexes.

The νCN vibration at 1472 cm^{-1} also shifts to 1461 cm^{-1} on Cl/Br substitution. This band appears at 1514 cm^{-1} after deuteration of the Hg(DTO)Cl_2 complex. The νCC band appears as a weak IR but very intensive Raman band at 945 cm^{-1} for the Cl complex and shifts to 936 cm^{-1} for the Br complex. The νCS vibration at 813 cm^{-1} doesn't shift on halogen substitution and appears at 727 cm^{-1} for the deuterated compound.

The bands in the region below 350 cm^{-1} are assigned in accordance with the results of the Hg(NN'DMDTO)X_2 complexes.

Hg(TMDTO)X_2

Table 5 summarizes the IR and Raman assignments for the Hg[$(CH_3)_2NCSCSN(CH_3)_2$]X_2 (X = Cl, Br, I) compounds. Figure 1 shows the IR and Raman spectrum of the Hg(TMDTO)Cl_2 complex.

The bands are assigned in accordance with the other HgLX_2 complexes (L = DTO, NN'DMDTO).

TABLE 3. Vibrational analysis of the Hg(NN'DMDTO)Cl_2 complexes

Hg(NN'$(CH_3)_2$DTO)Cl		Hg(NN'$(CH_3)_2$DTO)-Cl_2DEUT		Hg(NN'$(CD_3)_2$DTO)Cl_2		Hg(NN'$(CD_3)_2$DTO)-Cl_2DEUT		Assignment
IR	Raman	IR	Raman	IR	Raman	IR	Raman	
3155vs	3156vwvbr			3149vsbr				νNH
3059m-s	3027w			3031m-s				νNH
2964m-s	2967w	2964w						νCH_3
	2964m		2925vw					νCH_3
2899vw		2900vw		2900m-s				νNH
2890sh								
		2456w						
		2335m				2368m		νND
		2317m				2312m		νND
				2270vw		2272sh		νCD_3
				2229vw		2230sh		νCD_3
						2175sh		νCD_3
						2122sh		νCD_3
				2100vw		2098sh		νCD_3
				2050vw		2050sh		νCD_3
1549vs	1545vs	1521vs	1513s	1536vs	[1537]	1508vs	[1498]	νCN
1440sh	1443w	1440sh						δCH_3
1430m	1431w-m	1430m	1431w					δCH_3
1396vw		1400s	1398s		[1400]		[1398]	δCH_3
1376m				1377w				δNH
1361w	1365vvs	1361vw	1367m					δCH_3
1265vw	1269vw	1254vw						2 × [δNCS + νCS]
						1216m		
				1212w		1204m		2 × [δNCS + νCS]
						1195sh		2 × [δNCS + νCS]
1209m	1211sh	1207m	1203m	1177s	[1172]	1177m		νNR
1201m	1202m-s	1201m				1160w		νNR
1168w	1167w	1167vw	1154w	1136w-m		1135w		νNR
		1093m	1091w-m					ρCH_3
1093s	1092s	1063m	1065m	1110m		1079w		νCC
1063w-m	1063vw							ρCH_3
				1053m		1064w	[1062]	δCD_3
				1037m		1036w-m		δCD_3
1021w-m	1020w	1021w-m						ρCH_3
				983wbr	[989]	990vw		ρCD_3
						970w		ρCD_3
		931m	932w					δND
				890m-s		896w		ρCD_3
				882m-s		881vw		ρCD_3
873w-m	875w	850w-m	848w	847w-m		845s		νCS
						834sh		
807w-mbr	806vwbr			790w-mbr				πNH
727mbr				720mvbr				πNH
		691vw	695w-m			686w	[690]	
675w	674w-m	677w		670w		672w		ring vibration
634s	634ms	626s	627m	606s	[606]	601s	[602]	δNCS + νCS
603w	604w	602w		564w		567w		δNR
		562m				547wbr		πND
	529w							2 × νHgCl
		502w-m				499w		πND
391w-m	391w	388w-m	386w	362w	[364]	361w	[360]	πNR
346w-m	340sh	340w-m	335w	334w-m	[331]	329w-m	[330]	νHgS
333w	336w	335sh						ring def.
283sh								
267m	262w-m	266m	260w	270m	[260]	270m	[261]	νHgCl

(continued)

TABLE 3. *(continued)*

$Hg(NN'(CH_3)_2DTO)Cl$		$Hg(NN'(CH_3)_2DTO)$-Cl_2DEUT		$Hg(NN'(CD_3)_2DTO)Cl_2$		$Hg(NN'(CD_3)_2DTO)$-Cl_2DEUT		Assignment
IR	Raman	IR	Raman	IR	Raman	IR	Raman	
244m	254sh	245m	254w	245w-mbr		245mbr		νHgCl
189vw	188w							
				153w		153w		
148m	155w	148m	155w					lattice modes
				138w		138w		
106m	105sh	102m	107sh	104m	[105]	103m	[106]	lattice modes
					[89]			
81w-m	81vvs	81w-m	80vs	80w	[78]	81w	[77]	

TABLE 4. Vibrational analysis of the $Hg(DTO)X_2$ complexes

$Hg(H_2NCSCSNH_2)Cl_2$		$Hg(D_2NCSCSND_2)Cl_2$		$Hg(H_2NCSCSNH_2)Br_2$		$Hg(D_2NCSCSND_2)Br_2$		Assignment
IR	Raman	IR	Raman	IR	Raman	IR	Raman	
3186m				3243m				νNH_2
3036m				3142m				νNH_2
		2423m	2452w			2470s		νND_2
						2388vw		
		2249m				2332s		νND_2
1635s			1614s					δNH_2
						1589w		
		1554w	1556w-m			1547w	[1551]	
1472s	1488m	1514vs	1536w-m	1461s	1475m	1507vs		νCN
	1279m				1292m			ρNH_2
		1228w	1229vs				[1228]	$\delta ND_2 + \nu CC$
1181s			1174m					ρNH_2
		1133m				1129m		δND_2
		1035s				1041m		$\rho ND_2 + \nu CC$
945w	945vs	1020sh		936vw	936vs			νCC
813s	811vw			813s		812m		νCS
			774m				[772]	
		727s	725w			729s		νCS
739mbr				693m-s				$\omega,\tau NH_2$
		690vw	690vw					
674m	680m		660m	663s	677m	653m	[655]	$\delta NCS + \nu CS$
		575mbr	581vwbr					$\omega,\tau ND_2$
484m	485w	480w-m	483vw	464m		459m		ring vib.
		439w-m				423m		
376w	377vw		352w-m	367m	371m	342vw		ring def.
332m-s	324s	318m	300s	321m-s	332m	305s	[307]	νHgS
214w		210w						νHgCl
190sh	188m-s	192w	186mbr				[197]	
173w	173sh	171w	170sh	170sh	178m			ring def.
				162w		164w	[166]	νHgBr
				140w	145m-s	140m	[145]	νHgBr
128m		125m-s						δClHgCl
110sh	115s	110sh	114m					lattice modes
				102m		97w-m		δBrHgBr
90m	89m	89m	88w-m	86w-m	88m-s	82w-m		

In 'Experimental', we mentioned that the $HgLX_2$ complexes have to be pressed in KX pellets, where X is the same halogen as in the complex. In Fig. 2 the IR spectra of the $Hg(NN'DMDTO)Cl_2$ complex, pressed in KCl, KBr, KI and NaF respectively, are represented.

TABLE 5. Vibrational analysis of the Hg(TMDTO)X_2 complexes

X = Cl		X = Br		X = I		Assignment
IR	Raman	IR	Raman	IR	Raman	
3027vw	3030vw	3033vw	3031vw	3013vw	3013vw	νCH$_3$
2974vw	2975w	2975vw	2976w	2970vw	2071w	νCH$_3$
				2952sh		
2926vw	2933w-m	2928vw	2931w-m	2924w	2928w-m	νCH$_3$
	2906sh					
2850vw			2857sh	2855sh	2860sh	
	2794vw		2791vw	2789vw	2794vw	overtone
1570sh	1573s	1570vs	1572s	1568vs	1564s	νCN
1558vs	1564sh	1556vs	1563sh	1548vs	1555sh	νCN
1459w	1460w	1453sh	1454w-m	1451w		δCH$_3$
1443w	1443sh	1435w	1442sh	1437w	1449w	δCH$_3$
	1414s		1409s	1411sh	1409s	δCH$_3$
1402m-s	1401s	1404m-s	1398s	1401m	1400s	δCH$_3$
				1395s	1395sh	
1281s	1283w	1280s	1281w	1273m-s	1270m	ν_{as}RNR
			1278sh			
1263sh		1257sh		(1262sh)		
1241m	1244vw	1241w-m	1240vw	1241w-m	1240w	ν_{as}RNR
1189w	1190w	1189w	1187w	1184w	1183w	ρCH$_3$
1158w	1162w	1157w-m	1157w	1154w	1154w	ρCH$_3$
1120s	1124w	1119s	1122w	1114s	1112m	ρCH$_3$
			1116w			
1086w	1088vvw	1082sh		1082w	1083vw	ρCH$_3$
1051w	1053w	1051w-m	1052vw	1047w	1048vw	ρCH$_3$
971m	971w	969m	966w-m	969m	968w	νCC
960m	964w			960sh	959sh	
900vvw	899w-m	898vw	896w-m		896w-m	
		853w				
821w	822w	820s	820w	817m	816w-m	νCS
	640w	636w	636w-m	643w	642m	ν_sRNR
637vw	635w			627w	627w	ring vib.
620wbr	627vw	620w-m	622vw	620w	619w	ring vib.
562m	566m	563m	566m	569m	568m	δNCS + νCS
517w	519vvw	517w	517w	516w	515w	δRNR
438m	441w	436m	436w	430m	433w	δRNR
383w	383w	379w	380w	373w	371w	ring def.
350w	351w	346w-m	347w	336w	334w	νHgS
337w		332w-m	331vvw	323w	318w	νHgS
	297vs	288vw	290s		277w	
247sbr	251vs			257w	257m	νHgCl + ring def.
188vwbr	180m					
		174m-s	173vvs			νHgBr
	160m		159sh	165m	166vs	lattice modes
				141m	140vvs	νHgI
95wbr	103vvs			94w		

Pressed in KCl one becomes self-evidently the spectrum of the Hg(NN'DMDTO)Cl_2 complex.

When the Hg(NN'DMDTO)Cl_2 complex is pressed in KBr, the spectrum of Hg(NN'DMDTO)Br_2 occurs. The fact of halogen exchange can be proved by the position of the NH vibration and deformation bands. The νNH band shifts from 3154 to 3167 cm^{-1} and the πNH bands shift from 806 and 727 cm^{-1} to 781 and 701 cm^{-1} respectively. Also the νCN band shifts from 1549 to 1542 cm^{-1}. These results are in agreement with the results of the Zn(NN'DMDTO)Cl_2 complex [4].

By pressing the Hg(NN'DMDTO)Cl_2 complex in a KI matrix we tried to prepare the Hg(NN'DMDTO)I_2 complex, which could not be prepared in the normal preparative way. However, the spectrum of the ligand occurred. This can lead us to the conclusion that the I complex doesn't exist because of its instability,

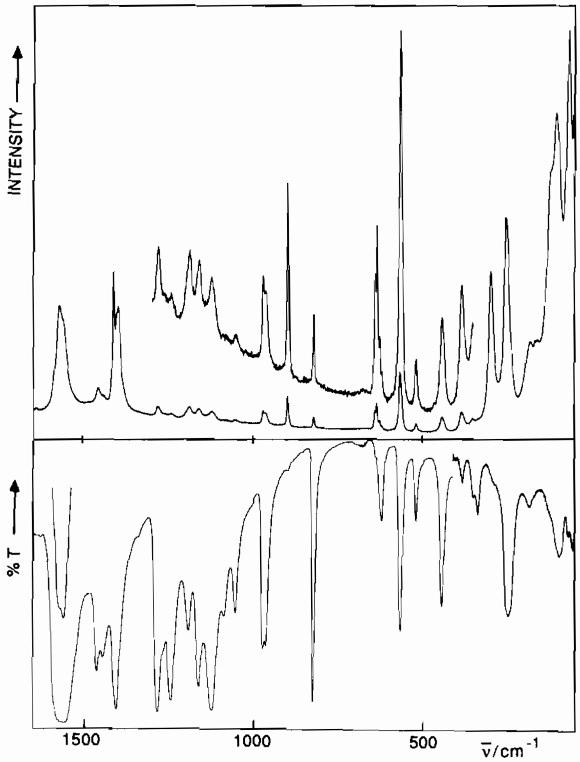

Fig. 1. The Raman and IR spectra of $Hg(TMDTO)Cl_2$.

which can be explained by the antisymbiotic effect (HSAB theory).

By pressing the Cl complex in a NaF matrix, the IR spectrum of a product analogue to the polymer, prepared by deprotonation in alkaline alcoholic medium [7] is observed, together with the bands of $NaHF_2$. This means that by pressing the NaF pellet, the $Hg(LH_2)F_2$ complex is formed, with exceptionally strong N–H···F hydrogen bonds. These hydrogen bonds result in the direct formation of HF and consequently in the formation of $NaHF_2$ and the deprotonated polymer complex $[HgL]_n$.

$$Hg(LH_2)Cl_2 + 2NaF \longrightarrow Hg(LH_2)F_2 + 2NaCl$$

$$Hg(LH_2)F_2 \longrightarrow HgL + 2HF$$

$$2HF + 2NaF \longrightarrow 2NaHF_2$$

Thermal Results

The thermal behaviour of the prepared complexes is characterized by different degradation mechanisms, depending on the ligands and on the halogens.

The TG curves of the $Hg(NN'DMDTO)X_2$ (X = Cl, Br) complexes are given in Fig. 3. For the Cl complex the formation of a horizontal mass plateau is observed while the Br complex shows only an inflection in the curve.

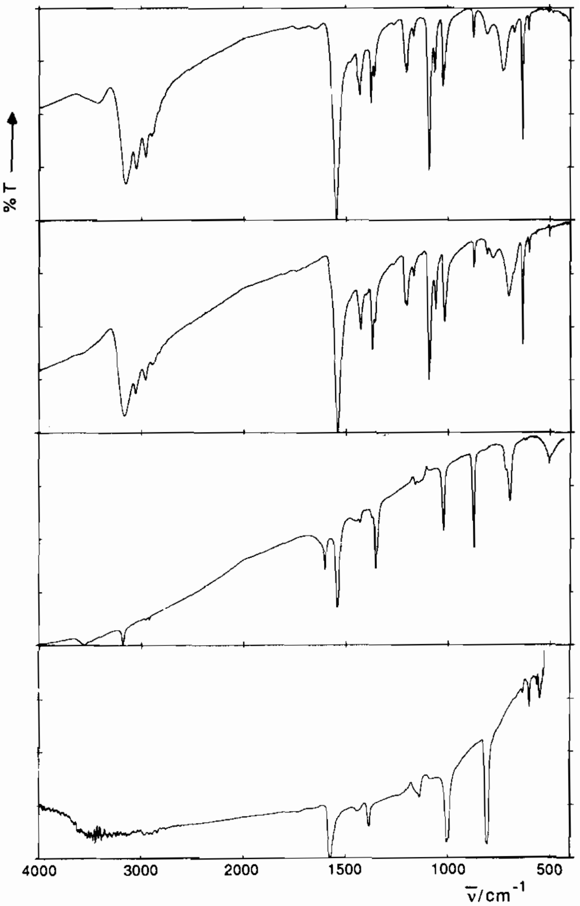

Fig. 2. The IR spectra of the $Hg(NN'DMDTO)Cl_2$ complex pressed in KCl, KBr, KI and NaF, respectively.

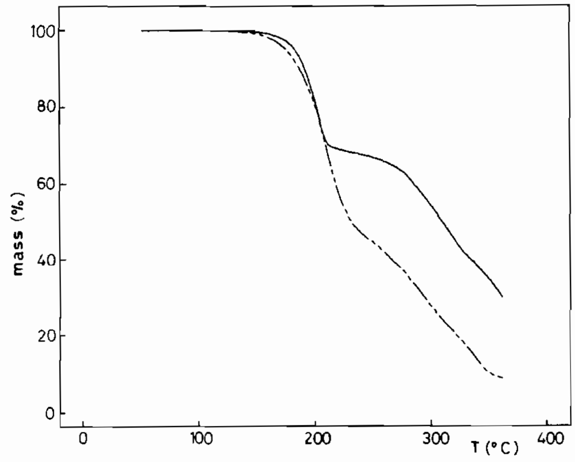

Fig. 3. The TG curves of the $Hg(NN'DMDTO)X_2$ complexes: ——, X = Cl; – · –, X = Br.

The MIR spectrum of the stable Cl intermediate shows the spectrum of the Hg(NN'DMDTO) deprotonated polymer form, which is in agreement with the $Zn(NN'DMDTO)Cl_2$ complex [8]. In accordance with the results of the Zn complex one can also prove that the Hg complex also loses a ligand as well as HCl on heating. The activation energy of the polymer formation is calculated by the variable heating rate method of Flynn and Wall [9]: E_a = (154 ± 2) kJ/mol.

Some intermediate complexes are unstable. However they can be isolated by keeping the rate of heating at 1 °C min^{-1} or in a more extreme way even by heating the complex isothermally. To become a stable Br complex intermediate the isothermal method at 100 °C was used. At this temperature the rate of mass loss is ±0.6% per hour and after a week there is a mass loss of ±80%. The IR spectra of the residue and of the product which sublimed in the glass oven tube both show the spectrum of Hg(NN'DMDTO)Br$_2$, so the conclusion is that the complex sublimes at this temperature. When the Br complex is heated in a non-isothermal way the complex will first sublime and at a certain temperature, indicated by the deflection point in the TG curve, the complex starts to decompose.

The TG curves of the Hg(DTO)Cl$_2$ and the Hg(DTO)Br$_2$ complexes differ completely from each other.

The curve of Hg(DTO)Cl$_2$ shows only one inflection point. The loss of mass at this point depends on the heating rate. The higher the heating rate, the higher the temperature of this point and the smaller the mass loss. The appearance of a point of inflection in the TG curve at a faster heating rate may resolve itself into a horizontal plateau at a slow heating rate; however the best approach to prepare a stable intermediate of this complex is to heat it isothermally. In contradiction with the Zn(NN'DMDTO)I$_2$ complex [8] the mass level is independent on the isothermal temperature (see Table 6). The higher the temperature, the higher the plateau. The MIR spectrum of the intermediate form cannot be identified. This is in agreement with the fact that the possibly formed Hg(DTO) deprotonated polymer form is an unstable one [7].

The curve of Hg(DTO)Br$_2$ (Fig. 4) shows four inflection points (three maxima and one shoulder in the DTG curve). It can be noticed that the first step is an exothermic one. The Figure also shows that there is a pH drop during the first and the third step. This pH drop is due to the loss of HBr. However, a clear view of the mechanism of the thermal degradation of Hg(DTO)Br$_2$ is not known.

TABLE 6. Relation between temperature of decomposition and horizontal mass level of Hg(DTO)Cl$_2$

Temperature (°C)	Mass level (%)
128	65.8
144	66.8
168	68.8
179	69.6
191	71.0

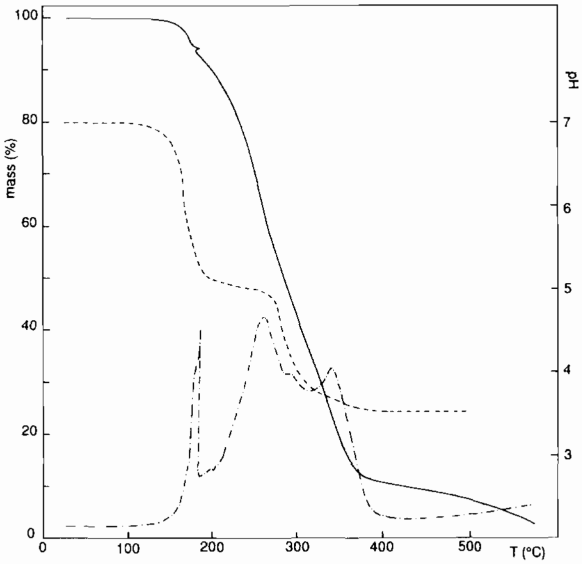

Fig. 4. The TG curve (——), the DTG curve (– · –) and the pH curve (- - - -) of the Hg(DTO)Br$_2$ complex.

TABLE 7. Activation energies (kJ/mol) for sublimation of the different products, calculated by the method of Flynn and Wall

	Hg(TMDTO)X$_2$	HgX$_2$
Cl	120 ± 4	86 ± 1
Br	111 ± 1	86 ± 3
I	97 ± 1	88 ± 1

The TG curves of the Hg(TMDTO)X$_2$ (X = Cl, Br, I) complexes are characterized by the fact that they show no inflection points. This is an indication for the fact that the complexes sublime upon heating. This can be proved unequivocally as the MIR spectrum of the product, which sublimed in the glass oven tube, agrees with the spectrum of the complex. The activation energies of sublimation for the three complexes are given in Table 7. The activation energies of the corresponding salts are also given in Table 7. It has to be noted that the activation energies of the complexes depend on the halogens while the E_a values of the salts are independent of X.

Conclusions

Based on spectroscopic evidence (νHgX values) and according to the literature data we propose a pseudotetrahedral structure [10–14] for the Hg(DTO)X$_2$ complexes and a distorted octahedral structure [15–19] for the Hg(NN′DMDTO)X_2 and the Hg(TMDTO)X_2 complexes.

The difference in intermolecular hydrogen bonding strength between the chloride, bromide and iodide complexes can be deduced from the position of the νNH or νNH_2 bands and even better from the position of the πNH or $\rho,\tau NH_2$ absorptions.

According to the HSAB theory the HgX bond strength increases on going from Cl → Br → I. Therefore the HgS bond strength and also the position of the νHgS vibration decreases according to the same series. For the complexes with L = DTO and NN′DMDTO the I complexes do not even exist. These complexes cannot be prepared in the normal preparative way nor by the halogen exchange by pressure reaction and this can be explained in terms of the antisymbiotic effect. As the HgS bond weakens when going from Cl to Br and further to I the CS bond becomes stronger but the νCS shift is not apparent as the νCS vibration is not pure. According to the same reasoning the CN bond strength should decrease on going from Cl → Br → I. This is in fact so as the νCN values decrease according to the same series.

The thermal degradation mechanisms differ for most of the complexes: some of the complexes sublime, some form polymers and some decompose by rather complex degradation mechanisms.

Acknowledgements

The authors wish to thank A. De Beleyr, J. Janssens, V. Van Heurck and G. Thijs for technical assistance.

References

1 A. C. Fabretti, G. C. Pellacani and G. Peyronel, *Gazz. Chim. Ital., 103* (1973) 1259.

2 A. C. Fabretti, G. C. Pellacani and G. Peyronel, *J. Inorg. Nucl. Chem., 36* (1974) 1751.

3 A. C. Fabretti, G. C. Pellacani and G. Peyronel, *Inorg. Nucl. Chem. Lett., 9* (1973) 897.

4 P. Geboes and H. O. Desseyn, *Spectrochim. Acta, Part A,* (1988) 963.

5 H. Hofmans, H. O. Desseyn and M. A. Herman, *Spectrochim. Acta, Part A, 38* (1982) 1307.

6 H. Hofmans, P. Geboes and H. O. Desseyn, *Spectrochim. Acta, Part A, 42* (1986) 969.

7 P. Geboes, B. Slootmaekers and H. O. Desseyn, *Spectrosc. Int. J., 6* (1988) 227.

8 P. Geboes, E. L. Esmans and H. O. Desseyn, *Thermochim. Acta, 124* (1988) 17.

9 J. H. Flynn and L. A. Wall, *Polym. Lett., 14* (1966) 323.

10 C. Marcotrigiano, *Z. Anorg. Allg. Chem., 422* (1976) 80.

11 G. B. Deacon, J. H. S. Green and D. J. Harrison, *Spectrochim. Acta, Part A, 24* (1968) 1921.

12 F. G. Moers and J. P. Langhout, *Recl. Trav. Chim. Pays-Bas, 92* (1973) 996.

13 J. M. Salas-Peregrin, *Can. J. Chem., 63* (1985) 3573.

14 T. Allman, R. G. Goel and P. Pilon, *Spectrochim. Acta, Part A, 35* (1979) 923.

15 R. J. H. Clark and C. S. Williams, *Inorg. Chem., 4* (1965) 350.

16 F. Cariati, G. Ciani, L. Menabue, G. C. Pellacani, G. Rossu and A. Sironi, *Inorg. Chem., 22* (1983) 1897.

17 J. E. Douglas and C. J. Wilkins, *Inorg. Chim. Acta, 3* (1969) 532.

18 A. C. Fabretti and G. Peyronel, *Spectrochim. Acta, Part A, 34* (1978) 667.

19 J. R. Ferraro, W. Wozniak and G. Roch, *Ric. Sci., 38* (1968) 433.